A High-Resolution Electron Momentum Spectroscopy and Density Functional Theory Study into the Complete Valence Electronic Structure of Allene

F. WANG,[1] H. MACKENZIE-ROSS,[2] D. A. WINKLER,[3] I. E. MCCARTHY,[2] L. CAMPBELL[2] and M. J. BRUNGER[2]

[1]*School of Chemistry, The University of Melbourne, Victoria 3010, Australia*
[2]*School of Chemistry, Physics and Earth Sciences, Flinders University of South Australia, GPO Box 2100, Adelaide, SA 5001, Australia*
[3]*Division of Molecular Sciences, CSIRO, Private Bag 10, Clayton South MDC, Victoria 3169, Australia*

Received 14 December 2000; accepted 5 February 2001

Dedicated to Professor Paul von R. Schleyer

ABSTRACT: A study of the electronic structure of the complete valence shell of allene (1,2-propadiene) is reported. New high-resolution binding-energy spectra were measured in the energy regime 6–34.5 eV over a range of different target electron momenta, so that momentum distributions (MDs) could be determined for each molecular orbital. These data supersede the low-resolution work of Braidwood et al. [J Phys B **27** (1994) 2075–2087], and also clarify some ambiguities with the earlier results. Theoretical MDs were calculated using a plane wave impulse approximation (PWIA) model for the reaction mechanism and density functional theory (DFT) for the wave function. Three basis sets, at the local spin density (LSD) approximation level and, additionally, incorporating nonlocal corrections such as the generalized gradient approximation (GGA), were studied. A critical comparison between the experimental and theoretical MDs was made, and it allowed us to determine the "optimum" wave function for allene from the basis sets we considered. This wave function is then used to derive allene's chemically interesting molecular properties. A summary of some of these results and a comparison of them with those of other workers is also presented with the level of agreement typically being good.
J Comput Chem 22: 1321–1333, 2001

Keywords: high-resolution; electron momentum spectroscopy; plane wave impulse approximation; density functional theory; momentum distributions

Correspondence to: M. J. Brunger; e-mail: michael.brunger@flinders.au.

This article includes Supplementary Material available from the authors upon request or via the Internet at ftp.wiley.com/public/journals/jcc/suppmat/22/13 or http://www.interscience.wiley.com/jpages/0192-8651/suppmat/v22.1321.html

Introduction

Allene (C_3H_4) or 1,2-propadiene, is an important organic reagent with structure $H_2C{=}C{=}CH_2$. As such, it is the simplest hydrocarbon to contain two double bonds. Interest in the electronic structure of allene, due in part to its unique ground-state molecular geometry,[1,2] prompted Braidwood et al.[3] to undertake the first electron momentum spectroscopy (EMS) study into its properties. Photoelectron spectroscopy (PES) interest in allene is also highlighted by the work of Baker and Turner,[4] Thomas and Thompson,[5] Bieri et al.,[6] Yang et al.,[7] and Baltzer et al.[8]

Braidwood et al.[3] measured binding-energy (ϵ_i) spectra of allene using their low-resolution noncoplanar symmetric electron-coincidence spectrometer. The energy resolution ($\Delta E_{\rm res}$) in that study was 1.40 eV, full width at half maximum (FWHM), and the angular resolution was 1.2° (FWHM). The total energy (E) was 1500 eV. The recoil momentum $\boldsymbol{p}$ was varied by varying the out-of-plane azimuthal angle ϕ over the angular range 0–30°. Binding-energy spectra were taken at each ϕ over the energy range ϵ_i = 8–40 eV using the binning mode.[9] From such spectra Braidwood et al.[3] derived momentum distributions (MDs) for the 2e, $1e + 2b_2 2a_1$, $1b_2$, and $1a_1$ valence molecular orbitals (MOs). Note that three independent measurements for the MDs were made by Braidwood et al., the MD data for each run being consistent with the results of the others for all MOs. Theoretical MDs were also calculated by Braidwood et al.[3] using a plane wave impulse approximation (PWIA) description for the ionization mechanism[9] and a Hartree–Fock (HF) wave function constructed from the GAMESS program.[10] Braidwood et al.[3] found only marginal agreement between their measured and calculated MDs with an illustrative and representative example of this for the 2e highest-occupied molecular orbital (HOMO) of allene being given in Figure 1. One possible reason for this discrepancy, between the theory and experimental MDs, was that their STO-3G basis was an inadequate representation for the 2e MO. Another possible explanation could be due to problems with their[3] binding-energy spectra measurements or in the spectral deconvolution procedure[11] employed by them to derive their MDs (see the Experimental section for more details). Indeed, Braidwood et al. noted some ambiguities with their work. For instance, they observed a "feature" in their binding energy spectra, centred at ϵ_f = 20 eV, which is not seen in any of the PES studies.[6,8] Such a "peak," which they had to include in their analysis to account for the measured coincidence signal in their binding-energy spectra, could arise due to either the low-energy resolution employed in their study, making the unique spectral deconvolution of overlapping features problematic, and/or as a result of employing Gaussian functions in their[3] spectral deconvolution, whereas the line profiles could in principle be quite asymmetric. Consequently, we have performed new high-resolution ($\Delta E_{\rm res} \sim 0.49$ eV FWHM) EMS measurements, under almost identical kinematical conditions as Braidwood et al. to resolve some of these ambiguities and also to provide a stringent crosscheck for the reported MDs. In addition, we also use the present measurements to investigate the validity of the spectroscopic sum rule[9] for allene.

In light of the marginal agreement between experiment and theory for the MDs, as found by Braidwood et al.,[3] Nicholson et al.[12] employed a numerical inverse method of extracting the target-ion overlap, or normalised Dyson orbital. This was specifically done for the 2e HOMO by using a quantum-mechanically constrained statistical fitting procedure. Again, the PWIA was used to describe the ionization mechanism with full details of this procedure being found in Nicholson et al.[12,13] The result[12] of employing the inverse method to the 2e experimental MD of Braidwood et al. is given in Figure 1. Clearly, their[12] present estimate of the normalised Dyson orbital provided a much better fit to the experimental 2e MD data than did that obtained using the GAMESS basis 2e orbital alone (see Fig. 1). This is well reflected by the value of χ^2 falling from 372, when the basis 2e HF STO-3G orbital is employed, to a value of 2.3 when the normalized Dyson orbital is used. As expected Nicholson et al. found the 2e basis orbital coefficient dominated the normalized Dyson orbital, the high-quality fit of Figure 1 being achieved with only a 6% 1e and unoccupied orbital contribution. Nonetheless, this 6% contribution is significant in another sense, as it clearly indicates the importance of electron-correlation effects in the allene molecule. Note that electron correlation effects, such as final-state-configuration-interaction,[9] do not invalidate the orbital-by-orbital MD analysis that we introduce later in this article. While correlation effects can potentially lead to a significant splitting of the manifold spectral strength into satellites,[9] thereby complicating the interpretation of the measured binding energy spectra, the MD of each satellite retains the same form as that for the manifold as a whole. Density Functional Theory (DFT), by its very

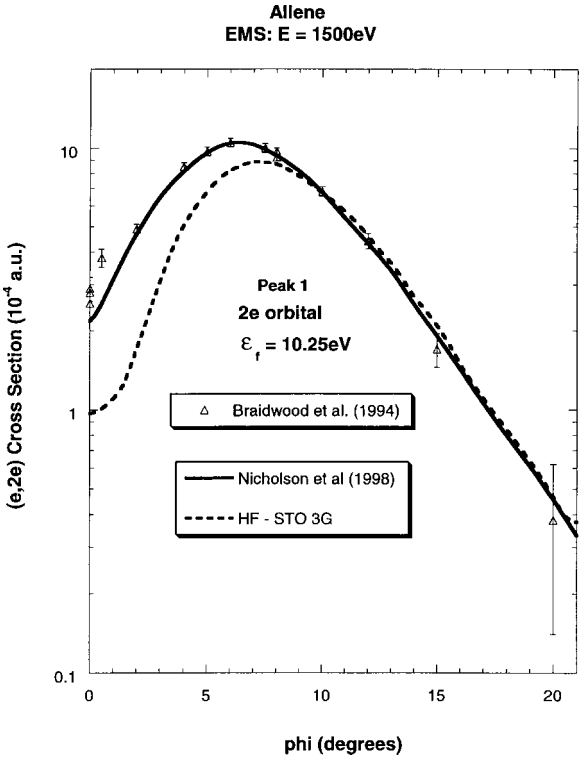

FIGURE 1. The 1500-eV symmetric noncoplanar momentum distribution for the 2e HOMO of allene. The data of Braidwood et al.[3] (Δ) is compared against the PWIA-SCF results of Braidwood et al.[3] (- - -) and the PWIA-normalized Dyson orbital result of Nicholson et al.[12] (—).

construction, already allows for electron-correlation considerations in the calculation of the Kohn–Sham orbitals.[14] Consequently, by using DFT basis sets we might determine PWIA-DFT MDs in better agreement with the present experimental results and those of Braidwood et al.,[3] than Braidwood et al. found earlier with their HF-level orbitals. We have, therefore, carried out DFT computations (see Theoretical Analysis section) to generate the molecular information required by the PWIA to calculate MDs for the valence MOs of allene. Three sets of DFT basis sets[15] at the TZVP, DZVP, and DZVP2 levels were employed in the present study. These calculations were carried out under the local spin density (LSD) approximation, both with and without nonlocal corrections. Full details of our calculations can be found in the Theoretical Analysis section of this article, with the present theoretical MD results and a comparison of them to the EMS data being given in the Comparison section.

The final significant aspect of the present application of high-resolution EMS is that by comparing the experimental and theoretical MDs, for the 2e, $1e+2b_2$, $2a_1$, $1b_2$, and $1a_1$ valence MOs, we can *a priori* independently determine which of the DFT basis sets we have studied provides the most physically reasonable representation of the allene molecule. We have previously seen[16–18] that such a procedure is highly sensitive in its ability to differentiate between the quality of various basis sets. Standard UniChem[19, 20] features then allow us to utilize this "optimum" wave function to extract the chemically important molecular property information for the allene system including bond lengths, bond angles, and infrared spectra. A selection of these data, along with a comparison of them with previous work, is given and discussed in the Molecular Property section of this article. Note that molecular property information determined in this way has also previously[16–18] been found to be in excellent agreement with values measured by independent experiments.

Experimental Details

The complete valence region of allene was studied in several experimental runs using the Flinders symmetric noncoplanar high-resolution electron momentum spectrometer.[21] A full description of the coincidence spectrometer, including the (e,2e) monochromator, and the method of taking the data can be found in Weigold and McCarthy[21] (and references therein) and so we do not repeat that detail again here.

The high-purity allene is admitted into the target chamber through a capillary tube, the flow rate being controlled by a variable leak valve. Note that the allene driving pressure was too low to cause any significant clustering by supersonic expansion. The collision region is surrounded by a chamber pumped by a 700 ls^{-1} diffusion pump. Apertures and slits are cut in the collision chamber for the incident beam and ejected electrons. The differentially pumped collision region makes it possible to increase the target gas density by a factor of about 3 while keeping the background pressure in the spectrometer below 10^{-5} Torr. This was important, as it enabled us to maintain workable coincidence count rate levels, even with the smaller electron beam current output from the (e,2e) monochromator (typically $\sim$25 μA) compared to that of a normal electron gun. The coincident energy resolution of the present measurements was 0.49 eV (FWHM), as determined from measurements of the binding-energy spectrum of helium. However, due to the

natural line widths of the various transitions (ranging from ~1 to 1.8 eV), as estimated from the relevant PES spectra,[6,8] the fitted resolutions of the spectral peaks for allene varied from 1.11 to 1.87 eV (FWHM). Nonetheless with the specified improvement in our coincident energy resolution (from 1.40 to 0.49 eV), we are now able to deconvolute with confidence the coincidence signals originating from the respective 2e, $1e + 2b_2$, and $2a_1$ outervalence orbitals and the signal arising from these orbitals and the innervalence $1b_2$ and $1a_1$ orbitals. This would not have been possible without the development of the (e,2e) monochromator.[22] Note that the coincidence signals arising from the 1e and $2b_2$ orbitals were summed in the present study to enable a direct comparison with the earlier low-resolution work of Braidwood et al.[3] The angular resolution was typically 1.2° (FWHM), as determined from the electron optics and apertures and from a consideration of the argon 3p angular correlation.

In the present investigation noncoplanar symmetric kinematics was employed, that is, the outgoing electron energies E_A and E_B are equal (750 eV), the two emitted electrons making equal polar angles $\theta = 45°$with respect to the direction of the incident electrons. The total energy (E), $E = E_0 - \epsilon_f = E_A + E_B$ was 1500 eV. The binding-energy range of interest (ϵ_f = 6–34.5 eV) is stepped through sequentially at each of a chosen set of angles ϕ using a binning mode[9] through the entire set of azimuthal angles (ϕ = 0–17.5°). Scanning through a range of ϕ is equivalent to sampling different target electron momenta $\boldsymbol{p}$ as

$$p = \left[(2p_A \cos\theta - 2p_0)^2 + 4p_A^2 \sin^2\theta \sin^2\left(\tfrac{1}{2}\phi\right)\right]^{1/2}. \quad (1)$$

For zero binding-energy ($\epsilon_f = 0$ eV), $\phi = 0°$ corresponds to $p = 0$ au, and for the present binding-energies, angular resolution and kinematics, $\phi = 0°$ corresponds to $p \sim 0.03$ au. Similarly for $\phi = 8°$, $p \sim 0.73$ au.

Typical binding-energy spectra for allene are given in Figure 2a and b. The solid curve in each panel represents the envelope of the 10 fitted Gaussians (various dashed curves) whose positions below $\epsilon_f \approx 25$ eV are taken from the available high-resolution PES data.[6,8] Above 25 eV, the positions of the Gaussians are taken from Braidwood et al.[3] Note that, specifically, in the binding-energy spectra peak 1 ≡ 2e orbital, peak 2 ≡ $1e + 2b_2$ orbitals, peak 3 ≡ $2a_1$ orbital and peaks 4–7 ≡ $1b_2$ and $1a_1$ orbitals. It is clear from Figure 2a and b that the fits to the measured binding-energy spectra are excellent. The least-squares fit deconvolution technique used in the analysis of these spectra is based on the work of Bevington and Robinson,[11] to whom inter-

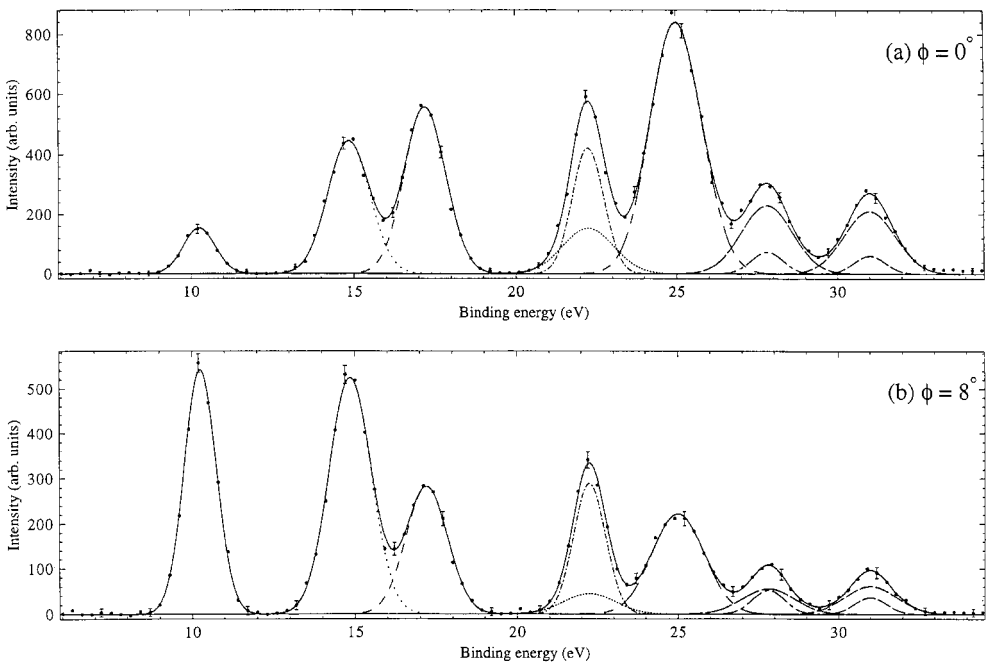

FIGURE 2. Typical binding-energy spectra from our 1500-eV noncoplanar symmetric EMS investigation into allene. The curves show the fits to the spectra at (a) $\phi = 0°$ ($p \sim 0.03$ au) and (b) $\phi = 8°$ ($p \sim 0.73$ au) using the known energy resolution.

ested readers are referred for more detail. The fact that the inner valence $1b_2$ and $1a_1$ orbitals needed 7 Gaussians to incorporate most of their measured coincidence intensity into the fit (consistent with Braidwood et al.[3] we measure additional $1b_2$ and $1a_1$ flux in the continuum $\epsilon_f > 33.5$ eV) is indicative for the existence of final state correlation effects in the inner valence region of allene. This hypothesis is entirely consistent with the results from the available many-body Green function method calculations.[3, 6, 8, 23]

There are, at this time, two further points we wish to highlight about the present high-resolution EMS binding energy spectra (Fig. 2). First, the present spectra are much cleaner, and all the features clearly better resolved than were found previously by Braidwood et al.[3] This should ensure unambiguous extraction of the experimental MDs for each orbital. Second, the present EMS binding-energy spectra are in excellent qualitative accord with the corresponding PES results.[6, 8] In particular, the present spectra show no "feature," centred at $\epsilon_f = 20$ eV, as did Braidwood et al.,[3] thereby resolving this ambiguity between the EMS and PES measurements.

Theoretical Analysis and Computational Details

The PWIA is used to analyze the measured cross sections for high momentum transfer (e,2e) collisions. Using the Born–Oppenheimer approximation for the target and ion wave functions, the EMS differential cross section σ, for randomly oriented molecules and unresolved rotational and vibrational states, is given by

$$\sigma = K \int d\Omega \left| \langle p\Psi_f^{N-1} \mid \Psi_i^N \rangle \right|^2 \qquad (2)$$

where K is a kinematical factor, which is essentially constant in the present experimental arrangement, Ψ_f^{N-1} and Ψ_i^N are the electronic many-body wave functions for the final [$(N-1)$ electron] ion and target [N electron] ground states, and p is the momentum of the bound electron at the instant of ionisation. The $\int d\Omega$ denotes an integral overall angles (spherical averaging) due to averaging over all initial rotational states. The average over the initial vibrational state is well approximated by evaluating orbitals at the equilibrium geometry of the molecule. Final rotational and vibrational states are eliminated by closure.

The momentum space target-ion overlap $\langle p\Psi_f^{N-1} | \Psi_i^N \rangle$ can be evaluated using configuration interaction (CI) descriptions of the many-body wave functions,[15] but usually the weak-coupling approximation[9, 21] is made. Here, the target–ion overlap is replaced by the relevant orbital of, typically, the Hartree–Fock or Kohn–Sham[14] ground state Φ_0, multiplied by a spectroscopic amplitude. With these two approximations, eq. (2) reduces to

$$\sigma = KS_j^{(f)} \int d\Omega \left| \phi_j(p) \right|^2 \qquad (3)$$

where $\phi_j(p)$ is the momentum space orbital. The spectroscopic factor $S_j^{(f)}$ is the square of the spectroscopic amplitude for orbital j and ion state f, and may be considered as the probability of finding the one-hole configuration in the many-body wave function of the ion.

The Kohn–Sham equation[14] of DFT may be considered as an approximate quasiparticle equation, with the potential operator approximated by the exchange–correlation (XC) potential.[15] Usually this is done at the local spin density (LSD) approximation level, although in this study we also employ nonlocal correlation functional corrections. To compute the coordinate space Kohn–Sham orbitals ψ_j we employed DGauss, a program package developed by CRAY Research by Andzelm and colleagues.[19, 20] DGauss is itself a part of UniChem, a suite of computational quantum-chemistry programs from Oxford Molecular. Using DGauss and UniChem, we employed various basis sets to build a model allene molecule and then we minimized the energy. The molecular coordinates at the optimum geometry (minimum energy) and the Gaussian molecular orbital parameters (coefficients and exponents) were next treated as input to the Flinders-developed AMOLD program,[9] which computes the momentum space spherically averaged molecular-structure factor[24] and the (e,2e) cross-section or momentum distribution (MD).

The comparisons of calculated momentum profiles with experiment (see the next section) may be viewed as an exceptionally detailed test of the quality of the basis set. In this investigation we have used three basis sets in the DFT computations. These basis sets are denoted by the acronyms DZVP, DZVP2, and TZVP. The notations DZ and TZ denote basis sets of double or triple ζ quality. V denotes a calculation in which such a basis is used only for the valence orbitals and a minimal basis is used for the less chemically reactive core orbitals. The inclusion of long-range polarization functions is denoted by P. The DZVP, DZVP2, and TZVP basis sets are especially designed for DFT calculations[19, 25] giving the respective contraction schemes of (621/41/1),

TABLE I.
Calculated Electronic Structure of the Allene Ground Electronic State Using Various DFT Functionals.

Method	Basis Set	R_{CC} (Å)	R_{CH} (Å)	∠HCC (°)	E (E_h)
GGA-BP	TZVP	1.311	1.094	120.962	−116.701196
GGA-BP	DZVP2	1.321	1.096	120.612	−116.684742
GGA-BWP	TZVP	1.311	1.094	120.962	−116.681426
GGA-BLYP	TZVP	1.312	1.092	121.015	−116.647641
GGA-WP	TZVP	1.309	1.092	121.012	−116.642647
SD-VWN	TZVP	1.302	1.098	120.028	−115.594469
HF-SCF[3]	STO-36[3]	1.308	1.082	120.0	−115.900785

The acronyms are explained in the text.

(721/51/1), and (7111/411/1) for carbon and (41), (41/1), and (3111/1) for hydrogen. Corresponding to these orbital basis sets are auxiliary basis sets to represent the electron density, the XC potential and energy. The auxiliary basis set corresponding to the DZVP, DZVP2, and TZVP orbital basis sets is called A2,[26] in which the s-, p-, and d-orbital exponentials were determined separately from an optimization that reproduces as accurately as possible the energy from an atomic DFT calculation. The contraction schemes of the A2 basis sets for H and C are (4/1) and (8/4/4), respectively.

The DFT calculations were performed using both the LSD and generalized gradient approximation (GGA) methods. The GGA methods use various gradient-corrected functionals based on the Becke–Perdew (BP) XC functionals—Becke[27] for exchange (X) and Perdew[28, 29] for the correlation (C) in the calculations. Other XC functionals such as the Becke–Wang–Perdew (BWP[30, 31]), Becke–Lee–Yang–Parr (BLYP[31]), and Wang–Perdew (WP) are also employed in the geometry optimizations. The LSD method invokes an LSD approximation using the Dirac exchange energy functional and the Vosko–Wilk–Nusair (VWN[32]) local spin density approximation level correlation energy functional. The calculations were performed on an SGI-2 work station and a CRAY J90se/82048 computer employing the computer distribution technique. Note that the term computer distribution technique is simply a shorthand notation to denote that the calculations were set up on the SGI-2 work station before being launched on the CRAY supercomputer.

Some of the results we have obtained, for the ground electronic state of allene, with the present basis sets and XC functionals are summarized in Tables I and II. It is clear from these tables that the calculated electronic structure and the calculated harmonic vibrational frequencies are rather sensitive to the basis set and XC functional used in the computation. Thus, a technique where *a priori* provides an indication for the most physically reasonable representation of the allene molecule, would be invaluable in determining which of the

TABLE II.
Calculated Harmonic Vibrational Frequencies (with Intensity > 1 km/mol) of the Allene Ground Electronic State Using Various DFT Functionals.[a]

Method	Basis Set	$\nu_1 = \nu_2$ (cm^{-1})	Int (km/mol)	$\nu_3 = \nu_4$ (cm^{-1})	Int (km/mol)	ν_9 (cm^{-1})	Int (km/mol)	ν_{11} (cm^{-1})	Int (km/mol)
GGA-BP	DZVP	372.493	9.43	769.529	59.56	1363.362	7.68	1998.840	87.48
GGA-BP	DZVP2	355.563	9.51	758.297	75.30	1364.290	8.98	1994.665	82.51
GGA-BP	TZVP	355.857	8.10	763.914	67.38	1374.987	6.51	1996.200	76.04
GGA-BWP	TZVP	374.635	9.05	775.795	59.81	1368.177	7.63	2000.022	85.52
GGA-BLYP	TZVP	368.465	8.63	775.420	57.49	1377.424	6.27	1985.142	83.12
GGA-WP	TZVP	372.440	9.29	774.253	61.85	1363.370	8.90	2007.746	87.30
SD-VWN	TZVP	387.600	11.36	774.750	65.75	1327.01	15.43	2034.130	104.32

[a] Zero-point vibrational energy is ≈33.4 kcal.

calculations was the most accurate. This point is explored further in the next section.

Comparison between Experimental and Theoretical Momentum Distributions

Typical binding-energy spectra of C_3H_4 in the region 6–34.5 eV and at $E = 1500$ eV are given in Figure 2. These spectra were measured at each of a chosen set of angles ϕ and then analyzed with a least-squares fit deconvolution technique.[11] This analysis allowed us to derive the required momentum distributions for all the respective valence orbitals of allene. Although the measured MDs are not absolute, relative magnitudes for the different transitions are obtained.[19] In the current EMS study the experimental momentum distributions were placed on an absolute scale using the same procedure as Braidwood et al.,[3] thereby allowing us to directly compare against their results.

Before examining, in turn, the momentum distributions for each of the valence MOs of allene, we make some general observations as to the results embodied in Figures 2–8. First, the typical binding-energy spectra of Figure 2 are in excellent qualitative agreement with the corresponding PES results.[6,8] There is no "feature," centered at $\epsilon_f = 20$ eV, observed in the present EMS binding-energy spectra, thereby resolving the ambiguity that had previously existed between the results of Braidwood et al.[3] and the PES studies.[6,8] Second, it is clear from Figures 3–8 that the present MDs and the earlier MDs of Braidwood et al. are in excellent agreement with one another for each of the respective valence MOs of allene and across all measured ϕ (or p). The present MDs, therefore, confirm the earlier results.[3] Finally, the current PWIA-DFT calculations are all in better agreement, again for each respective valence molecular orbital, with the present MD data and the MD data of Braidwood et al.,[3] than are the earlier PWIA-SCF (STO-3G) level calculations from Braidwood et al. This is specifically illustrated in Figures 1 and 3 for the 2e HOMO. Hence, the present DFT calculations provide a more physical representation for the allene molecule than did the earlier Hartree–Fock computation.[3]

In Figure 3 we compare our experimental MD, and that of Braidwood et al.,[3] for the 2e HOMO (at $\epsilon_f = 10.25$ eV) with the results from our PWIA-DFT computations for each of the three DFT basis states and five local/nonlocal XC functionals we have considered. We note that the errors on all the present experimental MDs, as derived during the deconvolution procedure, are one standard deviation uncertainties.[11] It is apparent from Figure 3 that all the present PWIA-DFT computations are in fair overall agreement with the measured MDs, the theory results somewhat underestimating the magnitude of the cross section for $1° < \phi < 6°$ and somewhat overestimating the magnitude of the cross-section for $\phi > 7.5°$. For this orbital it is not easy to differentiate between the quality of the various DFT calculations, they all lead to similar MDs (see Fig. 3) within a PWIA framework. However, on very close scrutiny, it is possible that the TZVP basis with BLYP and BP XC functionals give MDs in marginally better agreement with the experimental MD results, thus providing the best physical representation for the 2e orbital. All the PWIA-DFT calculations predict a local minimum in the MD at $\phi \approx 1°$. The present experimental MD results are not inconsistent with this theoretical prediction, which we believe originates from electron correlation effects.

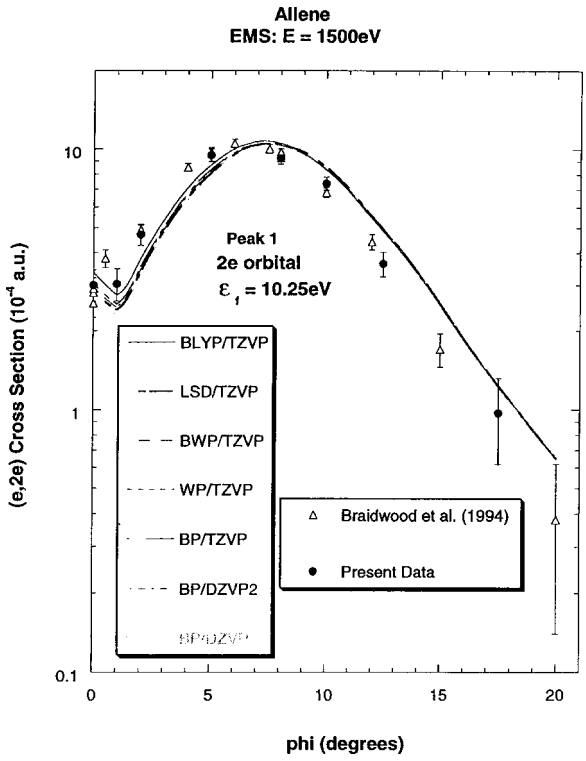

FIGURE 3. The 1500-eV symmetric noncoplanar momentum distribution for the 2e HOMO of allene. The present data (•) and the earlier data of Braidwood et al.[3] (Δ) are compared against the results of our PWIA–DFT calculations: (—) BLYP/TZVP, (- —) LSD/TZVP, (– –) BWP/TZVP, (- - -) WP/TZVP, (- - - -) BP/TZVP, (· – · –) BP/DZVP2, and (· · · · · ·) BP/DZVP. Acronyms are defined in the text.

The comparison between the PWIA-DFT and experimental MDs (present and Braidwood et al.[3]) is strong evidence for all the 2e spectroscopic strength being located at $\epsilon_f = 10.25$ eV. In other words the EMS measurements predict a spectroscopic factor $S_{2e} \sim 1$ at $\epsilon_f = 10.25$ eV. This observation is in excellent agreement with the results of the available many-body Green function calculations.[3, 6, 8]

PES measurements[4–6, 8] predict the 1e and $2b_2$ MOs to be essentially degenerate with ionisation potential ~15 eV. Consequently, we represent them in our spectral deconvolution procedure by a single Gaussian (under peak 2 of the binding-energy spectra) at $\epsilon_f = 14.85$ eV. The present experimental 1e + $2b_2$ MD, the 1e + $2b_2$ MD of Braidwood et al.[3] and our PWIA-DFT 1e + $2b_2$ MD calculation results are all plotted in Figure 4. Once again, the overall level of agreement between the theory and experimental MDs is fair and, like that described above for the 2e orbital, all the DFT basis sets lead to theoretical (e,2e) cross-sections that are very similar. The only exception to this general comment would appear to be the PWIA-DFT (BP/DZVP) result for $10° < \phi < 15°$, where it tends to overestimate the magnitude of the cross-section. The level of comparison between our experimental and theoretical MDs indicates that almost all the 1e and $2b_2$ spectroscopic fluxes have been identified under peak 2 of our binding-energy spectra. Thus, the present EMS spectroscopic factors for the 1e and $2b_2$ orbitals at $\epsilon_f = 14.85$ eV are both approximately one, i.e., $S_{1e} \sim 1$ and $S_{2b_2} \sim 1$ at $\epsilon_f = 14.85$ eV. These results are in very good agreement with the predictions of the many-body Green function calculations for the respective 1e and $2b_2$ orbitals.[3, 6, 8]

In Figure 5 the current $2a_1$ molecular orbital, at $\epsilon_f = 17.2$ eV, theoretical and experimental MDs are presented. Also shown in this figure are the previous MD measurements of Braidwood et al.[3] With the exception of the PWIA-DFT (LSD/TZVP and BWP/TZVP) MDs, which overestimate the magnitude of the (e,2e) cross-section at $\phi < 5°$, all the present calculations are in good agreement with the experimental MD data. Here it appears that most, if not all, of the $2a_1$ spectral strength is encompassed under peak 3 at $\epsilon_f = 17.2$ eV. Thus, the present EMS spectroscopic factor for the $2a_1$ orbital at $\epsilon_f = 17.2$ eV is $S_{2a_1} \sim 1$. Once again, this result is in good accord with those calculated using many-body Green function theories.[3, 6, 8]

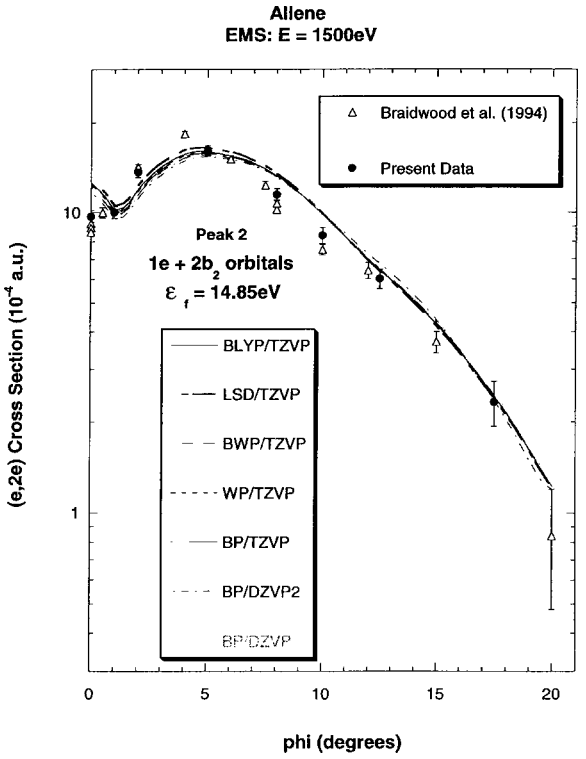

FIGURE 4. The 1500-eV symmetric noncoplanar momentum distribution for the 1e + $2b_2$ orbitals of allene. The legend is the same as that for Figure 3.

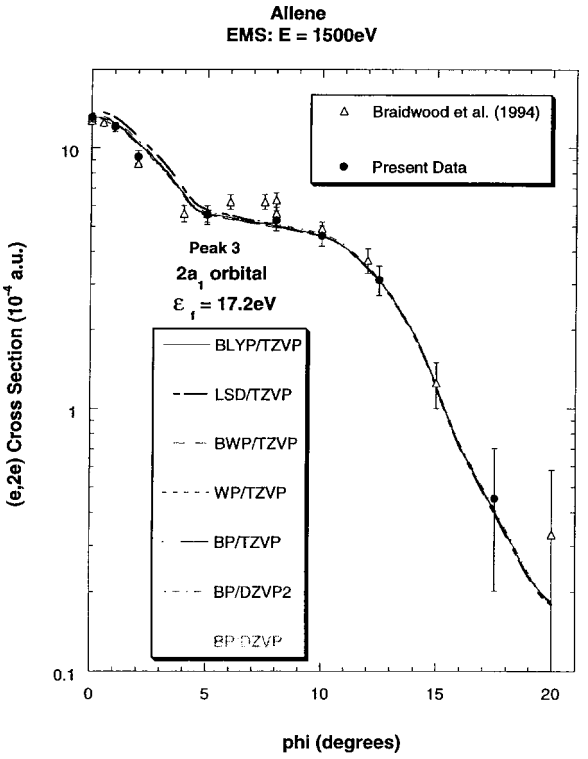

FIGURE 5. The 1500-eV symmetric noncoplanar momentum distribution for the $2a_1$ orbital of allene. The legend is the same as that for Figure 3.

We had previously noted that our binding-energy spectra, consistent with many-body theory predictions, indicated strong final-state configuration interaction effects for the inner valence orbitals, thereby leading to a splitting and mixing of the $1b_2$ and $1a_1$ spectroscopic strength. As a consequence of this, none of the current $1b_2$ PWIA-DFT MD calculation results are in agreement with the present experimental peak 4 MD or the corresponding MD of Braidwood et al., for $\phi < 12°$. In particular, the theory MDs overestimate the strength of the (e,2e) cross-section for $\phi < 4°$ and underestimate its magnitude for $5° \leq \phi < 12°$. This is clearly seen in Figure 6a. On the other hand, if we allow that under peak 4 of our binding energy, at $\epsilon_f = 22.25$ eV, there is an admixture of 67% of the total $1b_2$ spectral strength and 9% of the total $1a_1$ spectral strength, the level of agreement, except for the DZVP2/BP basis and XC functional, between our PWIA-DFT MD calculations and the measured MDs is very good. This is specifically illustrated in Figure 6b for the TZVP basis set and nonlocal BP exchange/correlation functional. Consequently, we can assign the spectroscopic factor of the $1b_2$ MO at $\epsilon_f = 22.25$ eV to be $S_{1b_2} \sim 0.67$, while the spectroscopic factor of the $1a_1$ MO at $\epsilon_f = 22.25$ eV is $S_{1a_1} \sim 0.09$.

Somewhat surprisingly, our spectral deconvolution indicated only a very small $1b_2$ contribution (<2%) under peak 5 of the binding-energy spectra. Consequently, most of the spectral strength under peak 5, at $\epsilon_f = 25.0$ eV, must originate from the $1a_1$ orbital. In Figure 7 we, therefore, plot our experimental $1a_1$ MD, the $1a_1$ MD from Braidwood et al.[3] and the results from our present PWIA-DFT calculations. As the inner valence $1a_1$ orbital is severely split by final-state configuration interaction effects,[3,6,8] we would anticipate our theoretical $1a_1$ results to overestimate the magnitude of the experimental cross-section for peak 5, particularly at small ϕ ($\phi < 5°$). This is exactly what is found in Figure 7. However, when the PWIA-DFT results are scaled by a factor of 0.51, good agreement between the experimental measurements and theoretical MDs, for $\phi \leq 5°$, is now found. This is illustrated in Figure 7 for the TZVP basis and BP-XC functional, but is

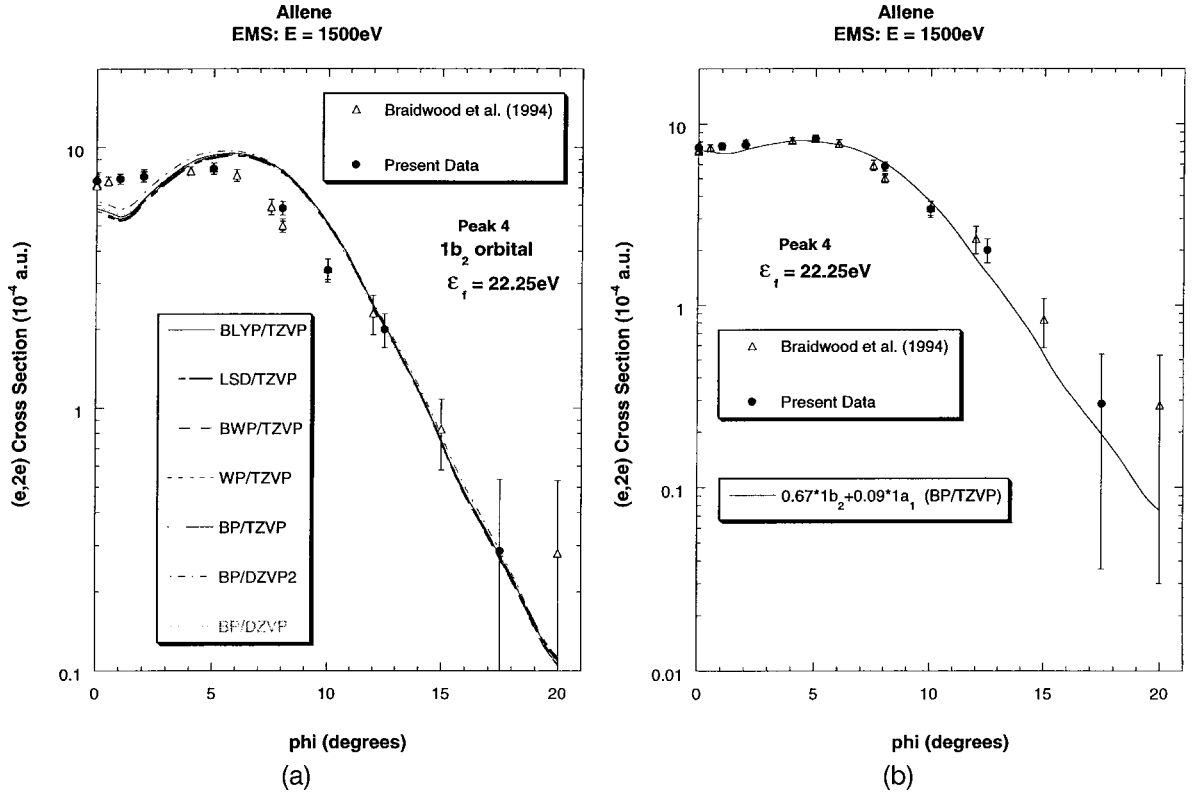

FIGURE 6. (a) The 1500-eV symmetric noncoplanar momentum distribution for the $1b_2$ orbital of allene. The legend is the same as that for Figure 3. (b) The 1500-eV symmetric noncoplanar momentum distribution for peak 4 ($\epsilon_f = 22.25$ eV) of the binding-energy spectra. The present data (•) and the earlier data of Braidwood et al.[3] (Δ) are compared against the result of our PWIA–DFT (BP/TZVP) calculation for $0.67 \times 1b_2 + 0.09 \times 1a_1$ (—).

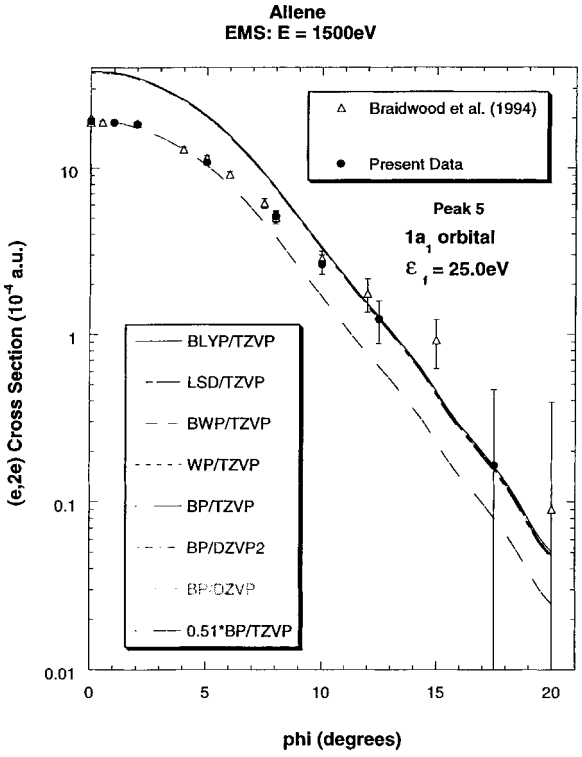

FIGURE 7. The 1500-eV symmetric noncoplanar momentum distribution for the $1a_1$ orbital of allene. The legend is the same as that for Figure 3 except $0.51 \times 1a_1$ (BP/TZVP) is additionally plotted (- - - -).

equally valid for all the basis states and exchange–correlation functionals we have studied. Hence, the spectroscopic factor for the $1a_1$ MO at $\epsilon_f = 25$ eV is $S_{1a_1} \sim 0.51$. Note that the agreement between our *scaled* PWIA-DFT results and the experimental MDs is still not perfect, the experimental cross section being larger in magnitude for $\phi > 5°$. From our previous experience[33] with tightly bound systems, i.e., inner valence and core states, this sort of behavior is consistent with the PWIA providing an inadequate description for the ionization mechanism. Under these circumstances[34] a multicentred distorted wave calculation (currently unavailable for molecules) would be necessary to correctly describe the collision dynamics. Consequently, the lack of agreement for $\phi > 5°$ between $0.51 \times$ PWIA-DFT $1a_1$ results and the experimental MDs is probably not a reflection of any serious limitation in our DFT basis states and XC functionals, rather it is a problem with the PWIA description of the reaction mechanism in this case.

Figures of the MDs for peaks 6, 7 and the continuum[3] are not plotted here, although in each case there is clear evidence for significant mixing of

TABLE III.
Allene Binding Energies (eV) and Spectroscopic Factors (in Parantheses) as Determined in the Present EMS Study.

Orbital	EMS	
2e	10.25 (∼1)	
1e	14.85 (∼1)	
$2b_2$	14.85 (∼1)	
$2a_1$	17.2 (∼1)	
$1b_2$	22.25 (∼0.67)	
	25.0 (<0.02)	
	27.8 (∼0.10)	(∼1)
	31.0 (∼0.09)	
	≥33.5 (∼0.10)	
$1a_1$	22.25 (∼0.09)	
	25.0 (∼0.51)	
	27.8 (∼0.14)	(∼1)
	31.0 (∼0.14)	
	≥33.5 (∼0.10)	

$1a_1$ and $1b_2$ spectral strength (see Table III). Rather, in Figure 8, we plot the MDs for the sum of the intensities under all of peaks 4–7 and the continuum (i.e., the cross-section for the $1b_2 + 1a_1$ orbitals), and the $1b_2 + 1a_1$ MD PWIA-DFT theory results. For $\phi < 10°$ the level of agreement between theory and experiment is very good, while for $\phi > 10°$ the experimental cross-sections are somewhat larger in magnitude than the corresponding calculations (see Fig. 8). Once again, we believe this discrepancy, at $\phi > 10°$, is due to limitations with the PWIA. Nonetheless, it is apparent from Figure 8 that all the $1b_2$ and $1a_1$ spectral strength has been accounted for under peaks 4–7 and in the continuum.[3] This is equivalent to saying that the spectroscopic factors for the respective $1b_2$ and $1a_1$ orbitals add up to 1, namely the spectroscopic sum rule for these molecular orbitals of allene has been validated.[21] This was, as noted earlier, also found to be the case for the 2e, $1e + 2b_2$, and $2a_1$ orbitals. All the present EMS binding energies and spectroscopic factors for each of allene's MO manifolds are summarized in Table III.

In our previous studies on 1,3-butadiene,[16] [1.1.1]propellane,[17] and cubane,[18] there were always experimental MDs, for one or two of the respective molecular orbitals, that could be used to make a clear distinction between the quality of the various basis sets and XC functionals that we employed in our DFT calculations.[35] Here, however, the situation is not so transparent. While it appears, on the basis of a comparison between the experimental and theory MDs, that TZVP provides a better physical rep-

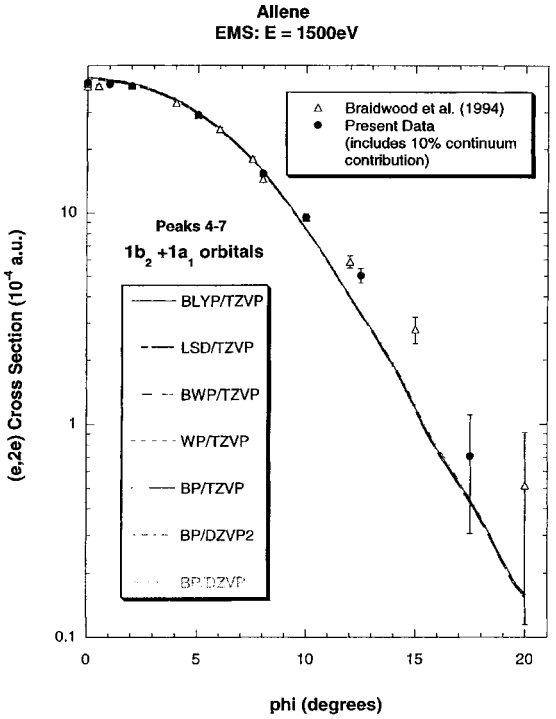

FIGURE 8. The 1500-eV symmetric noncoplanar momentum distribution for the $1b_2 + 1a_1$ orbitals of allene. The legend is the same as that for Figure 3. Note that a 10% continuum contribution ($\epsilon_f \geq 33.5$ eV), as determined by Braidwood et al.,[3] is allowed for in the present data.

resentation of the allene molecule than does either the DZVP or DZVP2 basis sets, it is less clear which of the nonlocal XC functionals (BLYP, BWP, WP, or BP) is superior, although all are better than the LSD level. Indeed, while a case could be made that the BLYP/TZVP and BP/TZVP DFT basis sets and XC functionals lead to MDs that are superior to those from the BWP/TZVP and WP/TZVP cases, it is impossible to distinguish between BLYP/TZVP and BP/TZVP simply on the MD comparisons alone. In this circumstance we must base our decision for the "optimum" DFT wave function of allene by relying on our past experience with other molecular systems[16–18] to choose the appropriate XC functional. Under this criterion our "optimum" DFT wave function for allene is BP/TZVP.

TABLE IV.
Bond Lengths and the HCC Bond Angle Calculated in This Work for Our "Optimum" Wave Function, Compared with Other Experimentally Determined Geometries.

Methods	r_e(C—C) Å	r_e(C—H) Å	∠HCC°
BP/TZVP	1.311	1.094	120.962
Microwave spectroscopy[2]	1.308	1.087	120.9
Microwave spectroscopy[1]	1.309	1.087	118.2

Molecular Property Information

Experimental validation of Hartree–Fock or density functional basis sets using EMS may provide a route to appropriate basis sets for calculating other types of molecular properties,[35] such as molecular geometries, NMR, vibrational spectra, and charge distributions etc. In this work we have taken our "optimum" DFT-BP/TZVP basis set and used it to derive some of these molecular properties. These are compared with experimentally determined values to see how well this optimum basis set was able to reproduce allene's molecular properties.

In general, our calculations of molecular geometric properties using the BP/TZVP XC functional and basis set are in very good agreement with the experimentally determined molecular properties.[1,2,4,7] The present results are summarized in Tables IV and V. In particular, the carbon–carbon bond distance of 1.311 Å from our calculations agreed very well with the two available[1,2]

TABLE V.
Harmonic Vibrational Frequencies (with Intensity >1 km/mol) Calculated in This Work for Our Optimum Wave Function, Compared with Other Experimentally Determined Values.

Methods	$\nu_1 = \nu_2$ (cm^{-1})	$\nu_3 = \nu_4$ (cm^{-1})	ν_9 (cm^{-1})	ν_{11} (cm^{-1})
BP/TZVP	355.857	763.914	1374.987	1996.200
Baker and Turner[4]	—	720	—	—
Yang et al.[7]	—	745	—	—
Hirota and Matsumara[1]	355.3	865	1398	1957

microwave spectroscopic method results of 1.308 and 1.309 Å, respectively. The present HCC bond angle of 120.962° was also in good agreement with that obtained by Maki and Toth[2] of 120.9°, both being somewhat larger than the value from Hirota and Matsumara[1] of 118.2°.

There have been a number of experimental determinations[1, 4, 7] of the vibrational spectrum of allene. These results are summarised in Table V, along with the results from our calculation with BP/TZVP. The current result for the ν_4 mode lies comfortably within the range for the experimentally determined values,[1, 4, 7] and is in particularly good accord with the value from Yang et al.[7] Similarly, the results for the ν_1, ν_9, and ν_{11} modes of Hirota and Matsumara[1] are also in quite good accord with our corresponding BP/TZVP results (see Table V).

Conclusions

We have reported a comprehensive theoretical and experimental EMS study into the complete valence electronic structure of allene. New high-resolution binding energy spectra for allene have been measured, and new DFT level calculations performed. Momentum distributions for the 2e, 1e + $2b_2$, $2a_1$, $1b_2$, and $1a_1$ molecular orbitals were derived and compared against an extensive series of PWIA-based calculations using DFT basis sets and various XC functionals. On the basis of this comparison, and from the calculated total energies of the various basis sets and nonlocal exchange correlation functionals used, we found the BP/TZVP result provided the most physically reasonable representation of the allene molecule. Molecular property information derived from this "optimum" basis and XC functional was found to be in good agreement with available results from independent measurements.

In addition, EMS spectroscopic factors for the valence MOs of allene were derived. The spectroscopic flux in each orbital manifold was found to be fully accounted for, so that the spectroscopic sum rule[21] was validated. Important final-state configuration interaction effects, for the inner valence states, were observed. This result is consistent with those from many-body Green function calculation techniques.

Acknowledgments

This article is dedicated to Professor Paul von Schleyer on the occassion of his 70th birthday. M.J.B. thanks the Flinders University of South Australia for some financial assistance so that he could attend Pacifichem 2000.

References

1. Hirota, E.; Matsumara, C. J Chem Phys 1973, 59, 3038.
2. Maki, A.; Toth, R. J Mol Spectrosc 1965, 17, 136.
3. Braidwood, S. W.; Brunger, M. J.; Weigold, E.; von Niessen, W.; Zakrzewski, V. G. J Phys B 1994, 27, 2075.
4. Baker, C.; Turner, D. W. Chem Commun 1969, 480.
5. Thomas, R. K.; Thompson, H. Proc Soc 1974, A339, 29.
6. Bieri, G.; Burger, F.; Heilbronner, E.; Maier, J. P. Helv Chim Acta 1977, 60, 2213.
7. Yang, Z. Z.; Wang, L. S.; Lee, Y. T.; Shirley, D. A.; Huang, S. Y.; Lester, W. A., Jr. Chem Phys Lett 1990, 171, 9.
8. Baltzer, P.; Wannberg, B.; Lundqvist, M.; Karlsson, L.; Holland, D. M. P.; MacDonald, M. A.; von Niessen, W. Chem Phys 1995, 196, 551.
9. McCarthy, I. E.; Weigold, E. Rep Prog Phys 1991, 54, 789.
10. Schmidt, M.; Baldridge, K. K.; Boatz, J. A.; Jensen, J. H.; Koseki, S.; Gordon, M. S.; Nguyen, K. A.; Windus, T. L.; Elbert, S. T. QCPE Bull 1984, 14, 52.
11. Bevington, P. R.; Robinson, D. K. Data Reduction and Error Analysis for the Physical Sciences; McGraw-Hill Inc.: New York, 1990.
12. Nicholson, R. J. F.; McCarthy, I. E.; Brunger, M. J. Aust J Phys 1998, 51, 691.
13. Nicholson, R. J. F.; McCarthy, I. E.; Weyrich, W. J Phys B 1999, 32, 3873.
14. Kohn, W.; Sham, L. Phys Rev 1965, 140, A1133.
15. Casida, M. Phys Rev A 1995, 51, 2005.
16. Brunger, M. J.; Winkler, D. A.; Michalewicz, M. T.; Weigold, E. J Chem Phys 1998, 108, 1859.
17. Adcock, W.; Brunger, M. J.; Clark, C. I.; McCarthy, I. E.; Michalewicz, M. T.; von Niessen, W.; Weigold, E.; Winkler, D. A. J Am Chem Soc 1997, 119, 2896.
18. Adcock, W.; Brunger, M. J.; McCarthy, I. E.; Michalewicz, M. T.; von Niessen, W.; Wang, F.; Weigold, E.; Winkler, D. A. J Am Chem Soc 2000, 122, 3892.
19. Andzelm, J.; Wimmer, E. J Chem Phys 1992, 96, 1290.
20. Komornicki, A.; Fitzgerald, G. J. J Chem Phys 1993, 98, 1398.
21. Weigold, E.; McCarthy, I. E. Electron Momentum Spectroscopy; Kluwer Academic/Plenum: New York, 1999, Chap. 2.
22. Hewitt, G. B.; Cottrell, G.; Northeast, R.; Utteridge, S.; Brunger, M. J. Meas Sci Technol, in preparation.
23. Cederbaum, L. S.; Domcke, W.; Schirmer, J.; von Niessen, W.; Diercksen, G. H. F.; Kraemer, W. P. J Chem Phys 1978, 69, 1591.
24. McCarthy, I. E.; Weigold, E. Rep Prog Phys 1988, 51, 299.
25. Godbout, N.; Salahub, D. R.; Andzelm, J.; Wimmer, E. Can J Chem 1992, 70, 560.
26. Dunlap, B. I.; Connolly, J. W. D.; Sabin, J. R. J Chem Phys 1979, 71, 4993.
27. Becke, A. D. Phys Rev A 1988, 38, 3098.

28. Perdew, J. P. Phys Rev B 1986, 33, 8822.
29. Perdew, J. P. In Electronic Properties of Solids 91; Akademie Verlag: Berlin, 1991.
30. Perdew, J. P. Phys Rev B 1992, 46, 6671.
31. Lee, C.; Yang, W.; Parr, R. G. Phys Rev B 1988, 37, 785.
32. Vosko, S. H.; Wilk, L.; Nusair, M. Can J Phys 1980, 58, 1200.
33. Brunger, M. J.; Braidwood, S. W.; McCarthy, I. E.; Weigold, E. J Phys B 1994, 27, L597.
34. Brunger, M. J.; McCarthy, I. E.; Weigold, E. Phys Rev A 1999, 59, 1245.
35. Adcock, W.; Brunger, M. J.; Michalewicz, M. T.; Winkler, D. A. Aust J Phys 1998, 51, 707.